HHS Public Access

Author manuscript

*Stem Cell Res*. Author manuscript; available in PMC 2017 March 01.

Published in final edited form as:

*Stem Cell Res*. 2016 March ; 16(2): 358–364. doi:10.1016/j.scr.2016.02.018.

# A 3D Culture System Enhances the Ability of Human Bone Marrow Stromal Cells to Support the Growth of Limbal Stem/Progenitor Cells

**Sheyla González**, **Hua Mei**, **Martin N. Nakatsu**, **Elfren R. Baclagon**, and **Sophie X. Deng**

Cornea Division, Stein Eye Institute, University of California, Los Angeles, CA, USA

## Abstract

The standard method of cultivating limbal epithelial progenitor/stem cells (LSCs) on a monolayer of mouse 3T3 feeder cells possesses the risk of cross-contamination in clinical applications. Human feeder cells have been used to eliminate this risk; however, efficiency from xenobiotic-free cultures on a monolayer appears to be lower than in the standard method using 3T3 cells. We investigated whether bone marrow stromal cells (BMSCs), also known as bone marrow-derived mesenchymal stem cells, could serve as feeder cells for the expansion of LSCs in the 3-dimensional (3D) system. Primary single human LSCs on a monolayer of 3T3s served as the control. Very poor growth was observed when single LSCs were cultured on BMSCs. When LSC clusters were cultured on a BMSC monolayer (CC-BM), 3D culture system (3D CC-BM) and fibrin 3D system (fibrin 3D CC-BM), the 3D CC-BM method supported a greater LSC expansion. The 3D CC-BM system produced a 2.5-fold higher cell growth rate than the control ($p<0.05$). The proportion of $K14^+$ and $p63\alpha^{bright}$ cells were comparable to those in the control ($p>0.05$), whereas the proportion of $K12^+$ cells was lower ($p<0.05$). These results indicate that BMSCs can efficiently support the expansion of the LSC population in the 3D culture.

### Keywords

Limbal stem cells; bone marrow stromal cells; bone marrow derived-mesenchymal stem cell; corneal epithelium; limbal stem cell deficiency

## 1. Introduction

Limbal epithelial stem/progenitor cells (LSCs) reside at the sclerocorneal junction (limbus) deep at the limbal epithelial crypt or lacuna that presumably constitutes the LSC niche [1-3]. Damage to the LSCs and their niche leads to limbal stem cell deficiency (LSCD). When LSCD is severe, normal homeostasis of corneal epithelial cells is impaired, and patients experience recurrent or persistent epithelial defect, corneal neovascularization, and scarring

**Corresponding author**: Sophie X. Deng, M.D., Ph.D., Associate Professor, Stein Eye Institute, University of California, Los Angeles, 100 Stein Plaza, Los Angeles, CA 90095, Tel: 310-206-7202, Fax: 310-794-7906, deng@jsei.ucla.edu.

of the cornea that ultimately lead to functional blindness. Replenishing LSCs by transplantation of cultivated LSCs is an effective treatment to restore a normal cornel epithelial surface.

The standard protocol to cultivate LSCs is to seed single LSCs directly on a monolayer of mouse 3T3 fibroblasts [4]. The 3T3 cells may serve as surrogate niche cells secreting the necessary growth factors and cytokines that are important in the maintenance of LSCs. Efforts to culture LSCs have included the modification of the culture system to re-create the *in vivo* environment of the LSC niche and to avoid the use of animal components in the culture system [5-8]. This niche is thought to possess unique properties that provide a special microenvironment that regulates the LSCs [9, 10]. LSCs are in close proximity with their subjacent limbal stromal niche cells, which are presumed to be located mostly around and underneath the LSCs. Crosstalk among niche cells, extracellular matrix components, and soluble factors control the differentiation cues to replenish the cornea epithelium during normal homeostasis and upon injury.

In some studies, LSC expansion efficiency was not optimal in a feeder-free system. Moreover, xenobiotic-free cultures appeared to have a lower clinical success rate than did the cultures using 3T3 feeder cells [11-13]; this reduction in clinical success could be due to the culture system not generating a sufficient number of LSCs.

To maintain the LSC phenotype *in vitro*, the culture conditions would need to replicate the LSC microenvironment *in vivo*. Bone marrow stromal cells (BMSCs), also known as bone marrow-derived mesenchymal stem cells, could serve as feeder cells to cultivate LSCs because BMSCs secrete factors required for epithelial cells proliferation, such as hepatocyte growth factor and keratinocyte growth factor [14]. However, the efficiency of LSC expansion using BMSCs has not been extensively evaluated. The proliferation rate and expression of markers that predict clinical outcome have not been measured [15].

Our laboratory has developed a novel 3-dimensional (3D) culture system that has been shown to be an efficient, consistent, and reproducible culture system to expand LSCs [8]. This 3D culture system allows LSCs to be in close proximity with feeder cells providing an even diffusion of growth factors and cytokines, and possible direct cell-to-cell contact between LSCs and feeder cells. The 3D system also addresses the following shortcomings of the traditional or standard 2-dimensional (2D) culture method: variation in nutrient diffusion results in nutrient gradients from the center of the LSC colonies to their periphery, and LSCs and feeder cells compete for the growth area in 2D systems.

In the present study, we compared several culture conditions, including our novel 3D culture method, to identify the optimal conditions in which BMSCs support the growth of LSCs.

## 2. Material & methods

### 2.1. Human sclerocorneal tissue

Human sclerocorneal tissues of 20- to 70-year-old healthy donors were obtained from several eye banks. Human tissue was handled in accordance with the tenets of the

Declaration of Helsinki. The experimental protocol was exempted by the University of California Los Angeles Institutional Review Board (IRB#12-000363). The tissues were preserved in Optisol™ (Chiron Ophthalmics, Inc., Irvine, CA) at 4°C. The death-to-preservation time was less than 10 hours (h), and the time from death to experiment was less than 7 days.

### 2.2. Limbal epithelial cell isolation

Prior to the isolation of the limbal epithelial cells, the iris, endothelium, conjunctiva, and Tenon's capsule were removed from the sclerocorneal rim tissue. The rim was incubated in 2.4 U/mL of dispase II (Roche, Indianapolis, IN) at 37°C for 2 h in DMEM/F-12 (Ham) medium (Life Technologies, Carlsbad, CA). Epithelial cell sheets were then isolated by gentle scraping under the dissecting microscope. Single cells were obtained by incubation with 0.25% trypsin and 1 mM EDTA (Life Technologies) for 5 min, and cell clusters were obtained by gently pipetting multiple times to break the cell sheet into small cell clusters.

### 2.3. Feeder cell culture

3T3-J2 mouse fibroblasts (the Howard Green laboratory, Harvard Medical School) were cultured in DMEM (ATCC, Manassas, VA) supplemented with 10% bovine calf serum (BCS; Thermo Fisher Scientific, Waltham, MA). BMSCs purchased at passage 2 (StemCell Technologies, Canada) were cultured in α-MEM (Life Technologies) supplemented with 10% fetal bovine serum (FBS; Life Technologies). To prepare growth-arrested feeder layers, subconfluent 3T3s and BMSCs were incubated with 4 and 8 μg/mL of mitomycin C, respectively, for 2 h at 37°C; then, they were transferred at densities of $3 \times 10^4$ cells/cm$^2$ and $2.3 \times 10^4$ cells/cm$^2$, respectively, to a new culture dish. Maintenance of the BMSC phenotype at different passages was confirmed by both morphology and immunohistochemical analysis of markers expression.

### 2.4. Limbal epithelial cell culture

LSCs were culture under three different culture conditions: a 2-dimensional (2D) method, the 3-dimensional method (3D), and the fibrin 3D method (Figure 1). In each set of conditions, the culture medium was supplemental hormone epithelial medium (SHEM) that consisted of DMEM/F12 medium supplemented with 5% FBS, N2 supplement (Life Technologies), 2 ng/mL of epidermal growth factor (EGF; Life Technologies), 8.4 ng/mL of cholera toxin (Sigma-Aldrich; St. Louis, MO), 0.5 μg/mL of hydrocortisone (Sigma-Aldrich), 0.5% of dimethyl sulfoxide (DMSO; Sigma-Aldrich). Cells were grown at 37°C in an atmosphere of 5% $CO_2$ for 14 days. The medium was changed every 2 to 3 days.

In the 2D method (Figure 1A), LSCs (density of 300 cells/cm$^2$) in the form of single cells or cell clusters, were plated directly on a monolayer of 3T3 cells or BMSCs. Single LSCs cultured on 3T3 cells served as the control. Single LSCs cultured on BMSCs is referred to as “SC-BM” and clusters of LSCs on BMSCs is referred to as “CC-BM” in the rest of the manuscript.

In the 3D method (Figure 1B), clusters of LSCs and BMSCs were cultured on the opposite sides of a porous PET membrane as previously described [8, 16]. Briefly, BMSCs were

allowed to attach for 5-6 h on the bottom side of the PET membrane (1-μm pore size). Then, the inserts were placed upright, and the clusters of LSCs at the same density as above were seeded onto the inner side of the membrane. This method is referred to as “3D CC-BM.”

In the fibrin 3D method (Figure 1C), a thin layer of fibrin gel was used to coated the inner surface of the PET membrane. Clusters of LSCs were cultured in the same way as in the 3D method (Baxter, Deerfield, IL). This method is referred to as “fibrin 3D CC-BM.”

Images of cell cultures were taken with an inverted DMIL LED microscope (Leica Microsystems, Wetzlar, Germany) equipped with Insight 11.2 color mosaic digital camera (Spot Imaging Solutions, Sterling Heights, Michigan). The cell expansion rate was measured on the basis of the cell population doubling (PD), calculated as log2 (number of cells harvested/number of cells seeded).

The cell growth success rate was obtained by dividing the number of successful LSC growth attempts by the total number of attempts.

### 2.5. RNA isolation, reverse transcription, and quantitative RT-PCR

Feeder cells were first washed away from the culture plates to avoid contamination. LSCs were lysed and homogenized by using a shredding system (QIAshredder; Qiagen, Valencia, CA). Total RNA was extracted by using RNeasy Mini Kit (Qiagen). The quantity and quality of total RNA were assessed with a spectrophotometer (NanoDrop 1000; NanoDrop, Wilmington, DE). Total RNA with minimal degradation was subjected to DNase treatment (Ambion Inc, Austin, TX) according to the manufacturer's recommendations.

Total RNA was reverse-transcribed (Superscript II RNase H2 reverse transcriptase; Invitrogen). The relative abundance of transcripts was detected by quantitative (q) RT-PCR (Brilliant SYBR Green Master Mix, Mx3000p real-time PCR system; Stratagene, La Jolla, CA). Cycle conditions were as follows: the reactant was denatured for 20 seconds (s) at 95°C, and amplification was conducted for 40 cycles (temperatures in each cycle were 95°C for 3 s, 60°C for 20 s, and 72°C for 8 s). The fluorescence intensity of each sample was normalized in relation to that of the housekeeping gene, glyceraldehyde-3-phosphate dehydrogenase (GAPDH). The primers used for qRT-PCR are listed in Table 1.

### 2.6. Immunocytochemistry

Cytospin slides from cultured LSCs were prepared by using a cytocentrifuge (Cytofuge; Thermo Scientific, Waltham, MA) and subsequently stored at −20°C. The cytospin method was chosen over the whole mount staining so that quantification of different cell populations of the entire culture could be achieved. BMSCs seeded on 2-well chamber slides (Thermo Scientific) were also processed for immunostaining. Fixation was done with 4% paraformaldehyde (PFA) at room temperature (RT) for 10 min. Nonspecific binding sites were blocked, and the cells were permeabilized in phosphate-buffered saline (PBS, Life Technologies) containing 1% bovine serum albumin (BSA, Sigma-Aldrich) and 0.5% Triton X-100 (Sigma-Aldrich) for 30 min at RT. Cells were incubated with primary antibodies (Table 2) diluted in PBS with 1% BSA and 0.1% Triton X-100 overnight at 4°C. Incubation with secondary antibodies was done at RT for 1 h. Nuclei were labeled with Hoechst 33342

(4 mg/mL; Life Technologies) at RT for 15 min. Fluoromount medium (Sigma-Aldrich) was used for slide mounting.

Images were acquired by a confocal microscope (Confocal Laser Scanning Microscopy; Olympus, San Jose, CA) and an image capture and analysis system (Fluoview FV10-ASW 3.1 Viewer; Olympus).

Quantitation of the cells that expressed a high level of p63α (p63α$^{bright}$ cells) was performed with the Definiens Tissue Studio software (Larchmont, NY) following the previously reported criteria [17].

### 2.7. High-resolution light microscopy

The 3D CC-BM cultures were fixed in a mixture of 2% PFA (Electron Microscope Sciences, Hatfield, PA) and 2.5% glutaraldehyde (Electron Microscope Sciences), osmicated for 1 h and embedded in an Epon resin (Momentive Specialty Chemicals, Houston, TX). For light microscopy analysis of the cell sheet structure, 1-μm sections were stained with 1% toluidine blue (Sigma-Aldrich) and 1% sodium borate (Sigma-Aldrich). Images were taken under a light microscope Zeiss Axio Imager.A2 (Carl Zeiss). The limbal epithelial cell sheet structure and cell-to-cell contacts between the cultured LSCs and BMSCs were analyzed.

### 2.8. Statistical analysis

Data were analyzed by using the Mann-Whitney test. Graph bars are expressed as the mean ± standard error of the mean (SEM) from a minimum of three independent experiments using different human sclerocorneal tissue donors. Statistical significance was defined as $p<0.05$.

## 3. Results

### 3.1. Characterization of BMSCs

BMSCs at passages 5 and 6 were used to culture LSCs. To confirm the maintenance of their initial phenotype, BMSCs were characterized by immunocytochemistry at passages 3 and 8. At passage 8, BMSCs maintained the expression of CD105 and N-cadherin (Figure 2A&B), which are commonly used markers for the identification of BMSCs, and were negative for the hematopoietic markers CD34 and CD45 (Figure 2C&D). The spindle-shaped morphology was consistent with that of BMSCs (Figure 2E). BMSCs were negative for osteocalcin, adiponectin, and Sox9, which are markers of more differentiated BMSC lineages (osteogenic, adipogenic, and chondrogenic), respectively (Figure 2F-H). Our results indicate that the BMSC phenotype is maintained until passage 8.

### 3.2. Morphology of cultivated LSCs

Undifferentiated cultured LSCs are small and cuboidal as shown in the image of the control (Figure 3A&B). In the SC-BM culture, the limbal epithelial cells were large and squamous-like (two features of more differentiated epithelial cells; Figure 3C). Moreover, the cell growth success rate when single LSCs were used was lower than 50%. Single LSCs cultured in the 3D and fibrin 3D systems using BMSCs showed a more differentiated morphology

than did those in the control (data not shown). LSCs in the CC-BM culture maintained a small, cuboidal morphology at the edge of the cell growth; however, the cells were more differentiated in the middle of the outgrowth (Figure 3D). In the 3D CC-BM cultures, very compact and uniform outgrowths containing small and cuboidal limbal epithelial cells were observed (Figure 3E&F). The cultured LSCs in the fibrin 3D CC-BM cultures were not as homogenous as those in the 3D CC-BM cultures (Figure 3G&H). The 3D CC-BM culture system appeared to better maintain the undifferentiated limbal epithelial cells.

### 3.3. Expansion rate of LSCs

A 100% cell growth success rate was achieved in the control system (Table 3). The 3D CC-BM method achieved the second highest success rate for cell growth (87.5%); lower success rates were seen with the CC-BM method (66.67%), the fibrin 3D CC-BM method (50%), and the SC-BM method (37.5%). The cell expansion rate, which was indicated by comparison of PD in the experimental culture systems with that in the control, was 24.14% less for the SC-BM culture ($p$=0.06; Figure 3I). In general, LSCs cultured in the form of cell clusters had a better cell expansion rate, and this rate was comparable to that in the control system. Both CC-BM and 3D CC-BM methods, when compared with the control, resulted in a 8.62% ($p$=0.13) and 24.14% ($p$=0.14) increase in the PD rate, respectively (Figure 3I). The fibrin 3D CC-BM method yielded a lower rate of PD than did the control (17.2% decrease, $p$=0.71; Figure 3I). Although none of the experimental conditions were statistically different from the control, there was a trend for a slight increase in the 3D CC-BM culture condition.

Single LSCs cultured on BMSC feeder cells did not support the expansion of limbal epithelial cells with undifferentiated morphology. In addition, single LSCs cultured on BMSCs had a poorer expansion rate than LSCs cultured in clusters. Therefore, LSC clusters were used in the rest of the experiments.

### 3.4. Phenotype of cultivated LSCs

We analyzed mRNA expression of the putative limbal stem cell markers—the ATP-binding cassette sub-family G member 2 (ABCG2), ΔNp63, N-cadherin, and cytokeratin (K) 14—and the marker of mature epithelial cells—K12. Comparable mRNA levels of K14 were found in LSCs cultivated in the 3D CC-BM, fibrin 3D CC-BM, and control systems (all $p$>0.05; Figure 4A). The K12 mRNA level was significantly lower in LSCs cultured in the 3D CC-BM and fibrin 3D CC-BM systems than in the control (decrease of 33.72% [$p$=0.028] and 9.57% [$p$=0.0001], respectively; Figure 4A). A lower ΔNp63 mRNA level was detected in LSCs isolated from the 3D CC-BM cultures (a decrease of 33.63%, $p$=0.003) and fibrin 3D CC-BM cultures (45.16%, $p$=0.038) than in cells isolated from the control system (Figure 4A). LSCs expanded in the CC-BM culture system showed a reduction of 42.15% in the K14 mRNA level ($p$=0.0005). N-cadherin mRNA expression was higher in LSCs cultivated by the CC-BM ($p$=0.042) or 3D-fibrin CC-BM ($p$=0.0074) methods (Figure 4A). Because N-cadherin expression also increases in epithelial mesenchymal transition (EMT), it was difficult to determine whether the level of N-cadherin in cultured LSCs was due to EMT or an increase in the undifferentiated stem/progenitor cell population. Therefore, analysis of N-cadherin protein expression was not performed.

Because mRNA expression may not reflect protein expression, we next investigated the population of cultured LSCs that expressed K14, K12 and high levels of p63α protein to further quantify the undifferentiated stem/progenitor population and the mature cell population. Expression of p63α is found in both transient amplifying (TA) cells and stem cells. However, cells expressing high levels of p63α are usually located at the basal layer of the limbus where LSCs reside. Moreover, the only known predictor of successful clinical outcome is the percentage of the $p63\alpha^{bright}$ cells [15]. A significant reduction in the number of $p63\alpha^{bright}$ cells was found in the CC-BM culture ($p$=0.04; Figure 4B&C). However, compared with the control system, both the 3D CC-BM and fibrin 3D CC-BM cultures were able to generate similar percentages of $p63\alpha^{bright}$ cells (12.85% *vs.* 13.61% [$p$=0.250] and 11.02% [$p$=0.249], respectively; Figure 4B&C). The p63 mRNA levels were not consistent with the p63 protein levels in cultured LSCs.

No significant differences were found in the percentage of $K14^+$ cells among all three culture conditions that used BMSCs as feeder cells and the control (all $p$>0.05; Figure 4D). K14 protein expression was consistent with K14 mRNA expression.

No significant differences in the percentage of $K12^+$ cells were found among all culture conditions (all $p$>0.05; Figure 4E); however, the percentage of $K12^+$ cells was slightly higher among populations cultivated in the CC-BM cultures (3.54%, $p$=0.286), the 3D CC-BM cultures (2.29%; $p$=0.463), and fibrin 3D CC-BM cultures (3.43%, $p$=0.643) than in the control (0.86%, Figure 4E). Overall, such small proportions of $K12^+$ cells are not clinically significant.

Taken together, our results indicate that the 3D CC-BM method yielded a higher cell growth success rate, a higher cell growth rate, and a larger proportion of undifferentiated corneal epithelial stem/progenitor cells than did all other culture methods in which BMSCs were used as feeder cells.

### 3.5. Histology and cell-to-cell contacts in the 3D CC-BM method

To further investigate the structure of the limbal epithelial cell sheets cultured in the 3D system and to determine whether feeder cells and cultured limbal epithelial cells established cell-to-cell contact, we used high-resolution microscopy to inspect 300 PET membrane pores in the 3D culture system. The limbal epithelial cell sheet consisted of 2 to 3 layers of cells: a basal layer of cuboidal cells and 1 to 2 layers of suprabasal squamous cells (Figure 5A&B). Possible contacts between limbal epithelial cells and BMSCs were observed in 14.46% of the PET membrane pores, (Figure 5C&D). Cell processes projected from epithelial cells were more common than the ones projected from BMSCs (21.69% *vs.* 7.22%, respectively, $p$=0.04; Figure 5D).

## 4. Discussion

Several LSC culture systems have been developed to re-create the LSC niche *in vitro* and to avoid the cross-contamination with non-human feeder cells [5-8]. It has been suggested that feeder cells are required to maintain a stratified epithelial sheet and to regenerate a sufficient number of progenitor cells in culture [18]. In the present study, LSCs were cultured with

human BMSCs as feeder cells in different systems to determine whether these BMSCs were a suitable replacement of mouse 3T3 feeder cells. To compare the quality of different culture systems, we evaluated several parameters such as cell morphology, cell growth success rate, PD rate, the proportion of stem/progenitor cells, and the proportion of mature corneal epithelial cells.

Based on the quantifiable measures that we evaluated, we determined that single LSCs could not be efficiently cultured on BMSCs in each culture method tested since differentiation in these cultures was increased (p63α data not shown). This finding is consistent with a previous observation [14]. LSCs cultured in the form of cell clusters achieve a higher expansion efficiency of the progenitor cell population [19, 20]. In contrast, LSC clusters cultured in the 2D system produced cell outgrowths with a very heterogeneous morphology and a significantly low number of $p63\alpha^{bright}$ cells; the presence of large differentiated cells at the center of the outgrowth, away from the feeder cells, suggested that nutrients secreted by the BMSC feeder cells could not reach this central area. In addition, the cell growth success rate was significantly lower in the 2D culture methods regardless of whether LSCs were seeded as single cells or as cell clusters. In the cultures of successful growth, the size of cell outgrowths was small and the cell morphology was consistent with that of differentiated epithelial cells at the center of the colony. These observations suggest that BMSCs can partially support the growth of LSCs in a 2D culture system.

Apart from the insufficient nutrient supply, the 2D method has other disadvantages that need to be overcome if cells produced in this system are used in a clinical setting [8]. First, both LSCs and feeder cells compete for the growth surface; LSCs push away the feeder cells as they grow, and this competition for the growth area might lead to a decrease in the number of feeder cells and an insufficient nutrient supply. Second, cross-contamination with the feeder cells is possible because both types of cells are grown in direct contact. To avoid these shortcomings in the 2D culture method, the 3D method was developed; this method has been shown to support the LSC phenotype and increase the expansion rate when mouse 3T3 feeder cells are used [8].

LSCs grown in the 3D CC-BM system demonstrated the most homogeneous limbal epithelial morphology. The cultured epithelial cells were small and cuboidal in shape with very tight cell-to-cell junctions. The cell expansion rate and the percentage of $K14^{+}$ and $p63\alpha^{bright}$ cells in the 3D CC-BM system were equivalent to the control. Although p63α is expressed in both TA and stem cells, cells expressing high levels of p63α are usually located at the basal layer of the limbus where LSCs reside. Moreover, the only known predictor of clinical outcome is the percentage of the $p63\alpha^{bright}$ cells [15].

The proportion of $K12^{+}$ cells in the 3D system was comparable to the control. The differences did not reach statistical significance and such low levels were clinically negligible. Our finding supports the hypothesis that the 3D culture system is better than the standard 2D system in mimicking the *in vivo* spatial environment of LSCs [8]. In this 3D culture system, LSCs are evenly distributed and in close contact with BMSCs; this arrangement allows a more homogeneous niche support that is not present in the direct

method of culture. Moreover, cross-contamination with feeder cells is avoided in this 3D method.

There were discrepancies between the mRNA and protein levels of p63 and K12. It is known that the mRNA level does not always correlate with the protein level. In addition, protein expression rather than mRNA expression dictates the phenotype of the cells. A better correlation was found between the cell morphology and the expression of stem/progenitor cell markers such as p63α and K14 proteins. Several reasons could account for the poor correlation between mRNA and protein expression: post-transcriptional modification, the half-lives of proteins, and the amount of "noise" in both protein and mRNA experiments [21, 22].

We hypothesized that the fibrin 3D CC-BM system provides an advantage over the 3D CC-BM system: the fibrin-containing system was expected to yield LSCs suitable for direct transplantation because the carrier for transplantation is already included in the culture system and there is no need to further passage the cultured LSCs onto a cell carrier, which could change their phenotype [23]. However, the fibrin gel, although permeable, may hinder the diffusion of some molecules and block the cell-to-cell contact in the 3D CC-BM system. The cell expansion rates and the cell growth success rates were lower in the fibrin 3D system. Because the PET membrane used in the 3D systems provides an unobstructed flow of growth factors, this feature may account for a better growth of LSCs in the 3D CC-BM system without the fibrin gel. To ensure a high engraftment rate, these cultured LSCs would need to be transferred to a cell carrier for transplantation.

We found that the cell growth rate in the fibrin 3D CC-BM system was lower than that in the 3D CC-BM system without fibrin. Large cell clusters had greater difficulty in attaching to the culture surface; however, when they did attach, the cultured cells retained their undifferentiated phenotype better than did single cells. The different surface structure of the fibrin gel and the PET membrane may influence the initial attachment of the LSCs to the surface and subsequent growth.

The histological study to investigate the cultured LSC sheets in the 3D CC-BM culture showed that there was direct cell-to-cell contact between the cultured LSCs and BMSCs. No cell-to-cell contact has been described between the cultured LSCs and 3T3 feeder cells in the 3D culture system [8]. Differences in the behavior of 3T3 cells and BMSCs in the 3D method could be due to the fact that BMSCs tend to spread out more in culture than 3T3 cells do and have longer and thinner cell processes that could establish contact with epithelial cells on the other side of the PET membrane. Moreover, N-cadherin, which is expressed by BMSCs, might mediate the cell-to-cell contact between LSCs and their native niche cells *in vivo* [24]. It is possible that the cell-to-cell contact between the cultured LSCs and BMSCs was mediated by N-cadherin and that these cell-to-cell contacts in the 3D system may be beneficial for the expansion of LSCs *in vitro*.

## 5. Conclusion

Using the 3D culture method in the absence of fibrin, we found a reproducible, efficient, and consistent method to expand the LSC population in the presence of BMSCs as feeder cells. The product of this system is a safer graft for future application in a clinical setting.

## Acknowledgments

This work was supported by National Eye Institute grants (5P30EY000331 and 1R01EY021797), by a California Institute for Regenerative Medicine (TR2-01768 and BF1-01768), and an unrestricted grant from Research to Prevent Blindness. We thank Ms. Shannon Eddington for technical support.

## Abbreviations

| | |
|---|---|
| **ABCG2** | ATP-binding cassette sub-family G member 2 |
| **BCS** | bovine calf serum |
| **BMSCs** | bone marrow stromal cells |
| **BSA** | bovine serum albumin |
| **CC-BM** | clusters of LSCs on a monolayer of BMSCs |
| **CFE** | colony-forming efficiency |
| **FBS** | fetal bovine serum |
| **fibrin 3D CC-BM** | clusters of LSCs on fibrin with BMSCs in the 3-dimensional method |
| **GAPDH** | glyceraldehyde 3-phosphate dehydrogenase |
| **K** | keratin |
| **LSCs** | limbal stem cells |
| **PBS** | phosphate-buffered saline |
| **PD** | population doubling |
| **PFA** | paraformaldehyde |
| **SC-BM** | single LSCs on a monolayer of BMSCs |
| **SHEM** | supplemental hormone epithelial medium |
| **3D CC-BM** | clusters of LSCs on BMSCs in the 3-dimensional method |
| **3T3** | 3T3-J2 mouse fibroblasts |

## References

1. Dua HS, Shanmuganathan VA, Powell-Richards AO, Tighe PJ, Joseph A. Limbal epithelial crypts: a novel anatomical structure and a putative limbal stem cell niche. Br J Ophthalmol. 2005; 89:529–532. [PubMed: 15834076]
2. Shortt AJ, Secker GA, Munro PM, Khaw PT, Tuft SJ, Daniels JT. Characterization of the limbal epithelial stem cell niche: novel imaging techniques permit in vivo observation and targeted biopsy of limbal epithelial stem cells. Stem Cells. 2007; 25:1402–1409. [PubMed: 17332511]

3. Zarei-Ghanavati S, Ramirez-Miranda A, Deng SX. Limbal lacuna: a novel limbal structure detected by in vivo laser scanning confocal microscopy. Ophthalmic Surg Lasers Imaging. 2011; 42:e129–131. Online. [PubMed: 22150603]
4. Lindberg K, Brown ME, Chaves HV, Kenyon KR, Rheinwald JG. In vitro propagation of human ocular surface epithelial cells for transplantation. Invest Ophthalmol Vis Sci. 1993; 34:2672–2679. [PubMed: 8344790]
5. Sharma SM, Fuchsluger T, Ahmad S, Katikireddy KR, Armant M, Dana R, Jurkunas UV. Comparative analysis of human-derived feeder layers with 3T3 fibroblasts for the ex vivo expansion of human limbal and oral epithelium. Stem Cell Rev. 2012; 8:696–705. [PubMed: 21964568]
6. Xie HT, Chen SY, Li GG, Tseng SC. Isolation and expansion of human limbal stromal niche cells. Invest Ophthalmol Vis Sci. 2012; 53:279–286. [PubMed: 22167096]
7. Chen SY, Mahabole M, Tseng SC. Optimization of Ex Vivo Expansion of Limbal Epithelial Progenitors by Maintaining Native Niche Cells on Denuded Amniotic Membrane. Transl Vis Sci Technol. 2013; 2:1. [PubMed: 24222891]
8. Mei H, Gonzalez S, Nakatsu MN, Baclagon ER, Lopes VS, Williams DS, Deng SX. A three-dimensional culture method to expand limbal stem/progenitor cells. Tissue Eng Part C Methods. 2014; 20:393–400. [PubMed: 24047104]
9. Daniels JT, Harris AR, Mason C. Corneal epithelial stem cells in health and disease. Stem Cell Rev. 2006; 2:247–254. [PubMed: 17625261]
10. Li W, Hayashida Y, Chen YT, Tseng SC. Niche regulation of corneal epithelial stem cells at the limbus. Cell Res. 2007; 17:26–36. [PubMed: 17211449]
11. Sangwan VS, Basu S, Vemuganti GK, Sejpal K, Subramaniam SV, Bandyopadhyay S, Krishnaiah S, Gaddipati S, Tiwari S, Balasubramanian D. Clinical outcomes of xeno-free autologous cultivated limbal epithelial transplantation: a 10-year study. Br J Ophthalmol. 2011; 95:1525–1529. [PubMed: 21890785]
12. Shortt AJ, Bunce C, Levis HJ, Blows P, Dore CJ, Vernon A, Secker GA, Tuft SJ, Daniels JT. Three-year outcomes of cultured limbal epithelial allografts in aniridia and Stevens-Johnson syndrome evaluated using the Clinical Outcome Assessment in Surgical Trials assessment tool. Stem Cells Transl Med. 2014; 3:265–275. [PubMed: 24443006]
13. Zakaria N, Possemiers T, Dhubhghaill SN, Leysen I, Rozema J, Koppen C, Timmermans JP, Berneman Z, Tassignon MJ. Results of a phase I/II clinical trial: standardized, non-xenogenic, cultivated limbal stem cell transplantation. J Transl Med. 2014; 12:58. [PubMed: 24589151]
14. Omoto M, Miyashita H, Shimmura S, Higa K, Kawakita T, Yoshida S, McGrogan M, Shimazaki J, Tsubota K. The use of human mesenchymal stem cell-derived feeder cells for the cultivation of transplantable epithelial sheets. Invest Ophthalmol Vis Sci. 2009; 50:2109–2115. [PubMed: 19136703]
15. Rama P, Matuska S, Paganoni G, Spinelli A, De Luca M, Pellegrini G. Limbal stem-cell therapy and long-term corneal regeneration. N Engl J Med. 2010; 363:147–155. [PubMed: 20573916]
16. Nakatsu MN, Gonzalez S, Mei H, Deng SX. Human limbal mesenchymal cells support the growth of human corneal epithelial stem/progenitor cells. Invest Ophthalmol Vis Sci. 2014; 55:6953–6959. [PubMed: 25277234]
17. Di Iorio E, Barbaro V, Ferrari S, Ortolani C, De Luca M, Pellegrini G. Q-FIHC: quantification of fluorescence immunohistochemistry to analyse p63 isoforms and cell cycle phases in human limbal stem cells. Microsc Res Tech. 2006; 69:983–991. [PubMed: 16972233]
18. Miyashita H, Shimmura S, Higa K, Yoshida S, Kawakita T, Shimazaki J, Tsubota K. A novel NIH/3T3 duplex feeder system to engineer corneal epithelial sheets with enhanced cytokeratin 15-positive progenitor populations. Tissue Eng Part A. 2008; 14:1275–1282. [PubMed: 18433313]
19. Kawakita T, Shimmura S, Higa K, Espana EM, He H, Shimazaki J, Tsubota K, Tseng SC. Greater growth potential of p63-positive epithelial cell clusters maintained in human limbal epithelial sheets. Invest Ophthalmol Vis Sci. 2009; 50:4611–4617. [PubMed: 19324845]
20. Gonzalez S, Deng SX. Presence of native limbal stromal cells increases the expansion efficiency of limbal stem/progenitor cells in culture. Exp Eye Res. 2013; 116:169–176. [PubMed: 24016868]
21. Greenbaum D, Colangelo C, Williams K, Gerstein M. Comparing protein abundance and mRNA expression levels on a genomic scale. Genome Biol. 2003; 4:117. [PubMed: 12952525]

22. Maier T, Guell M, Serrano L. Correlation of mRNA and protein in complex biological samples. FEBS Lett. 2009; 583:3966–3973. [PubMed: 19850042]

23. O'Driscoll L, Gammell P, McKiernan E, Ryan E, Jeppesen PB, Rani S, Clynes M. Phenotypic and global gene expression profile changes between low passage and high passage MIN-6 cells. J Endocrinol. 2006; 191:665–676. [PubMed: 17170223]

24. Hayashi R, Yamato M, Sugiyama H, Sumide T, Yang J, Okano T, Tano Y, Nishida K. N Cadherin is expressed by putative stem/progenitor cells and melanocytes in the human limbal epithelial stem cell niche. Stem Cells. 2007; 25:289–296. [PubMed: 17008425]

## Highlights

- 3D CC-BM culture is more efficient at expanding LSCs than the standard 2D method
- 3D CC-BM culture avoids the risk of cross-contamination in clinical applications
- LSCs in the 3D CC-BM culture form 2 to 3 cell layers with cuboidal basal cells

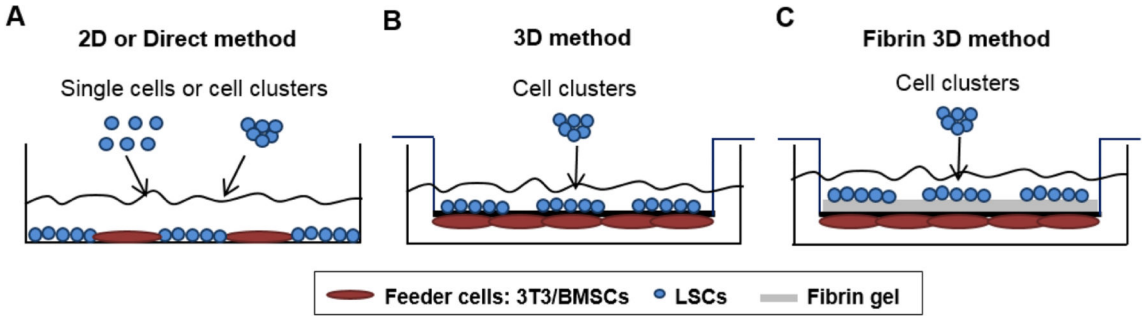


**Figure 1.**

Schematic representation of the different culture systems: the 2-dimensional (2D) method **(A)**, the 3-dimensional (3D) method (**B),** and the fibrin 3D method **(C)**.

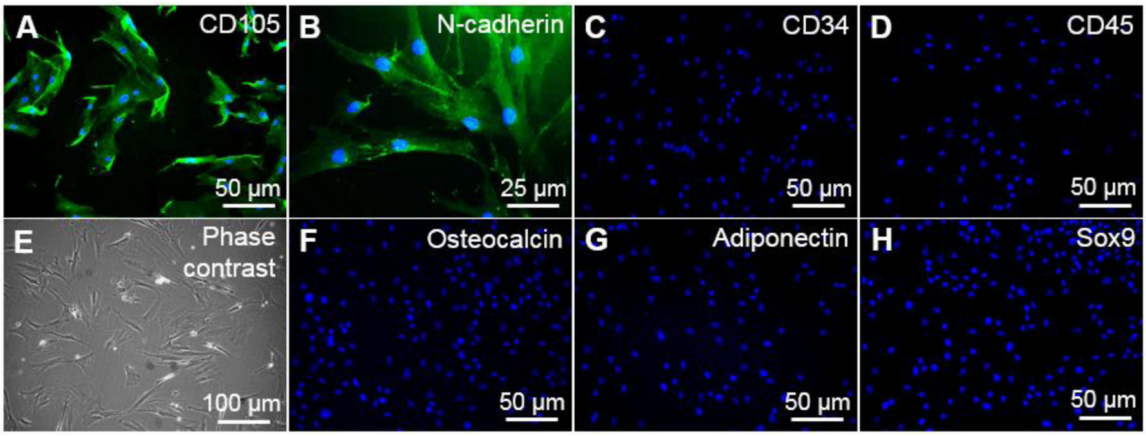


**Figure 2.**

Characterization of the BMSC line by immunocytochemical analysis of the following markers: CD105 **(A)**, N-cadherin **(B)**, CD34 **(C)**, CD45 **(D)**, osteocalcin **(F)**, adiponectin **(G),** and Sox9 **(H)**. The morphology of BMSCs was evaluated by phase contrast microscopy **(E)**.

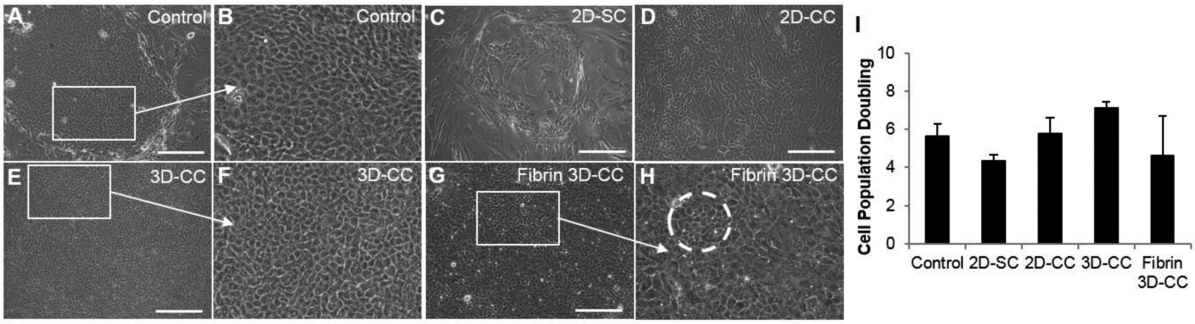


**Figure 3.**

Morphology *in vitro* and cell growth rate of LSCs in the different culture systems.

Morphology of the control **(A, B)**, 2D-SC **(C)**, 2D-CC **(D)**, 3D-CC **(E, F)**, fibrin 3D-CC **(G, H)** and cell population doubling **(I)**. The dashed circle in H indicates clusters of cells with a LSC-like morphology. Scale bar indicates a distance of 100 μm.

Abbreviations: 2D-SC, single LSCs in the direct system with BMSCs; 2D-CC, LSC clusters in the direct system with BMSCs; 3D-CC, LSC clusters in the 3D system with BMSCs; fibrin 3D-CC, LSC clusters in the fibrin 3D system with BMSCs.

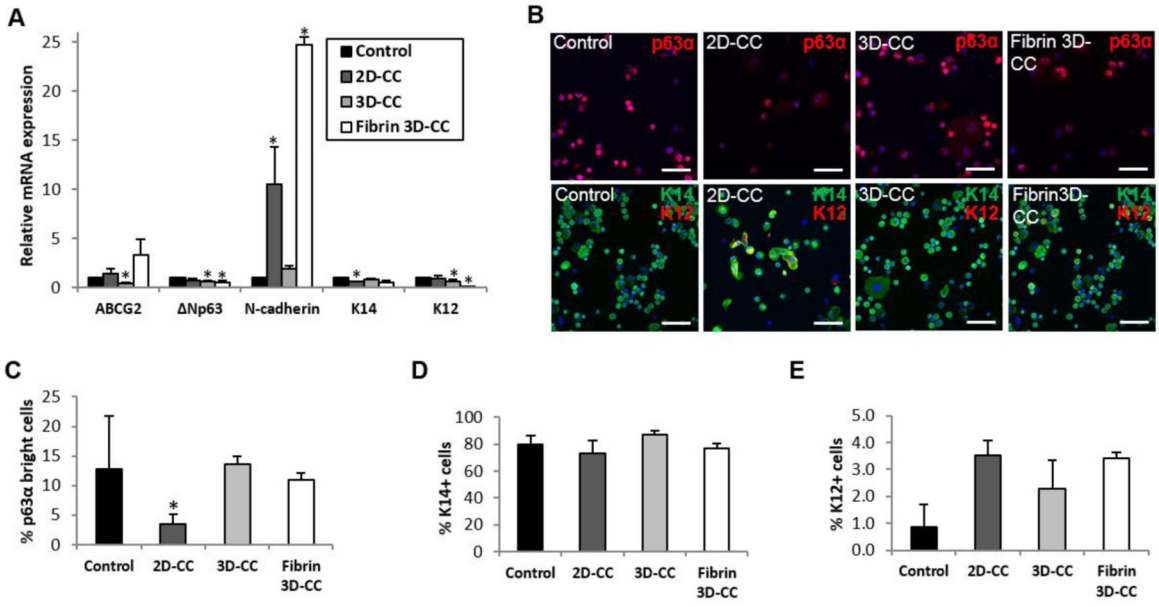


**Figure 4.**

Phenotype of cultured LSCs in the different culture systems. Expression at the mRNA level of the putative limbal stem cell and differentiation markers **(A)**. Representative results of p63α and K14-K12 immunocytochemical analysis **(B)**. The scale bar indicates a distance of 100 μm. Quantitation of $p63\alpha^{bright}$ cells **(C)**. Quantitation of $K14^{+}$ cells **(D)**. Quantitation of $K12^{+}$ cells **(E)**.

Abbreviations: 2D-CC, LSC clusters in direct method with BMSCs; 3D-CC, LSC clusters in 3D method with BMSCs; fibrin 3D-CC, LSC clusters in fibrin 3D method with BMSCs.

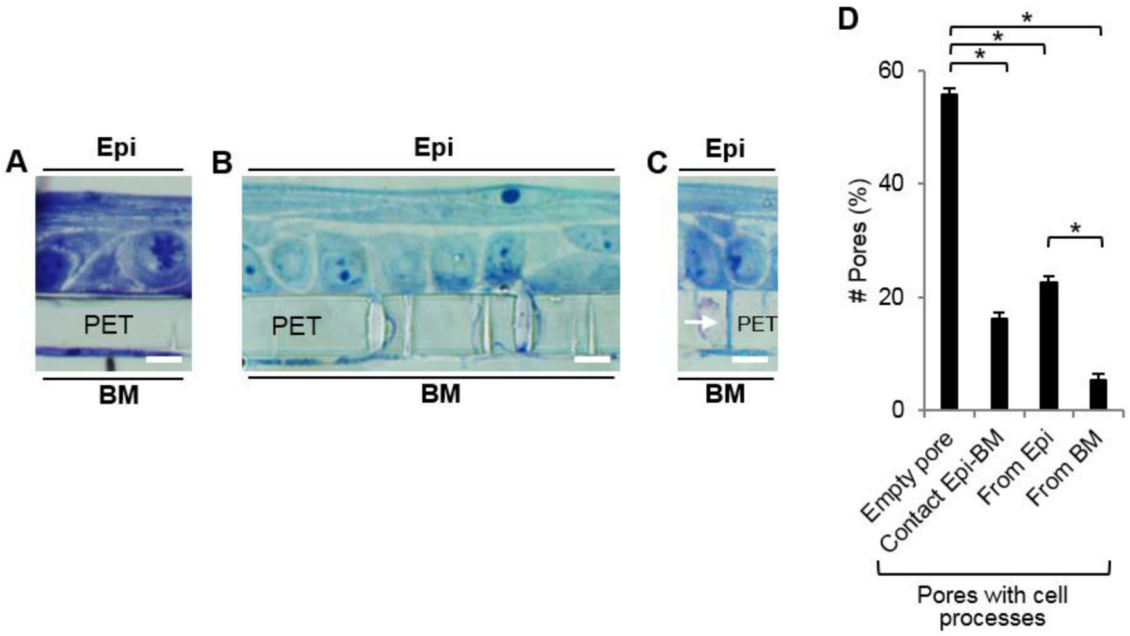


**Figure 5.**

High-resolution light microscopy of the limbal epithelial cell sheets in the 3D CC-BM culture. Limbal epithelial cell sheet and BMSCs on both sides of the PET membrane **(A)**. Morphology of the limbal epithelial cell sheet (top of the PET membrane) **(B)**. Possible cell-to cell contact between epithelial and BMSCs (arrow) **(C).** Quantitation of PET membrane pores with and without possible cell contact **(D)**. Scale bar indicates a distance of 10 μm. Abbreviations: BM, bone marrow stromal cells; Epi, epithelium; PET, polyethylene terephthalate.

## Table 1

Primers used for qRT-PCR.

| Gene | Direction | Primer Sequence (5'→3') | GeneBank Accession number |
|---|---|---|---|
| GAPDH | Forward | CGACCACTTTGTCAAGCTCA | NG_007073.2 |
| | Reverse | AGGGGTCTACATGGCAACTG | |
| ABCG2 | Forward | CCGCGACAGCTTCCAATGACCT | NG_032067.2 |
| | Reverse | GCCGAAGAGCTGCTGAGAACTGTA | |
| ΔNp63 | Forward | TCCATGGATGATCTGGCAAGT | NG_007550.1 |
| | Reverse | GCCCTTCCAGATCGCATGT | |
| N-cadherin | Forward | GAGGAGTCAGTGAAGGAGTCA | NG_011959.1 |
| | Reverse | GGCAAGTTGATTGGAGGGATG | |
| K14 | Forward | GACCATTGAGGACCTGAGGA | NG_008624.1 |
| | Reverse | ATTGATGTCGGCTTCCACAC | |
| K12 | Forward | CCAGGTGAGGTCAGCGTAGAA | NG_008077.1 |
| | Reverse | CCTCCAGGTTGCTGATGAGC | |
| Ki67 | Forward | CTTTGGGTGCGACTTGACG | NC_000010.11 |
| | Reverse | GTCGACCCCGCTCCTTTT | |

ABCG2, ATP-binding cassette sub-family G member 2; GAPDH, glyceraldehyde-3-phosphate dehydrogenase; K12, cytokeratin 12; K14, cytokeratin 14.

**Table 2**

Primary antibodies used for immunocytochemistry.

| Primary Antibody | Dilution | Source and Catalogue # |
|---|---|---|
| K12 | 1:100 | Santa Cruz Biotechnology sc-25722 |
| K14 | 1:50 | Fisher Scientific MS-115-R7 |
| p63α | 1:100 | Cell Signaling Technology #4892 |
| N-cadherin | 1:50 | Santa Cruz Biotechnology sc-8424 |
| CD105 | 1:100 | Abcam ab114052 |
| CD34 | 1:100 | Abcam ab6330 |
| CD45 | 1:100 | eBioscience 14-0459-82 |
| Osteocalcin | 1:100 | Abcam ab13421 |
| Adiponectin | 1:100 | Abcam ab113943 |
| Sox9 | 1:100 | Abcam ab118892 |

K12, cytokeratin 12; K14, cytokeratin 14.

**Table 3**

Cell growth success rate of LSCs from different culture systems.

| Group | Successful growth | Total | % |
|---|---|---|---|
| Control | 10 | 10 | 100.00 |
| CC-BM | 6 | 9 | 66.67 |
| 3D CC-BM | 7 | 8 | 87.50 |
| Fibrin 3D CC-BM | 4 | 8 | 50.00 |